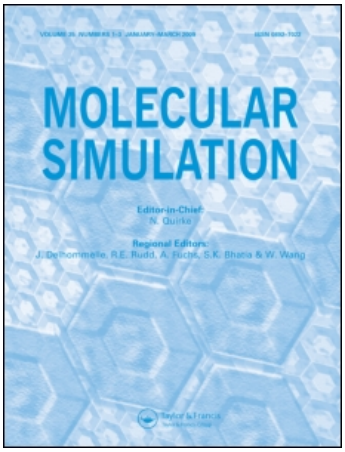

Molecular Simulation
Publication details, including instructions for authors and subscription information:
http://www.informaworld.com/smpp/title~content=t713644482

Structures and Energetics of Platinum-Cobalt Bimetallic Clusters

Yu Hang Chui[a]; Kwong-Yu Chan[a]
[a] Department of Chemistry, The University of Hong Kong, Hong Kong SAR, P.R. China

To cite this Article Chui, Yu Hang and Chan, Kwong-Yu(2004) 'Structures and Energetics of Platinum-Cobalt Bimetallic Clusters', Molecular Simulation, 30: 10, 679 — 690
To link to this Article: DOI: 10.1080/08927020412331279929
URL: http://dx.doi.org/10.1080/08927020412331279929

Molecular Simulation, Vol. 30 (10), 30 August 2004, pp. 679–690

Taylor & Francis
Taylor & Francis Group

Structures and Energetics of Platinum–Cobalt Bimetallic Clusters

YU HANG CHUI and KWONG-YU CHAN*

Department of Chemistry, The University of Hong Kong, Pokfulam Road, Hong Kong SAR, P.R. China

(Received June 2004; In final form June 2004)

Platinum–cobalt bimetallic clusters ($N = 11–15$) were modeled by a many-body Sutton-Chen (SC) potential. The basin-hopping algorithm and Monte Carlo (MC) energy minimization were used to determine the global minima of bimetallic clusters. The structural changes with cluster size were observed. Most of the structures had built on icosahedral packing. Second energy difference analyzes were performed to investigate the relative stability of a cluster with respect to its size and composition. The dependence of energetics and structures on size and composition is discussed.

Keywords: Platinum–cobalt bimetallic cluster; Basin-hopping algorithm; Sutton-Chen potential; Nanoclusters

INTRODUCTION

Nanoparticles of pure metals and mixed metals are of interest in medicine, catalysis, as well as electromagnetic applications. Experimental techniques such as, vibrational spectroscopy and microscopy are limited in achieving spatial resolution in the atomic scale. Theoretical studies can complement experimental approaches and provide understanding of nanomaterials in the atomic scale. Cagin, Goddard and co-workers [1–4] reported the thermal and mechanical properties of some transition metals and alloys and the melting and crystallization of nickel nanoclusters. Nayak *et al.* [5–7] investigated the thermodynamics, energetics and equilibrium geometries of small nickel clusters. Wales and co-workers [8–11] used the Sutton-Chen (SC) potential to calculate the structures, dynamics and global energy minima of transition metal clusters. Shiang and co-workers [12–13] studied atomic diffusion on the surface of metals. Huang and Balbuena studied platinum nanoclusters on graphite substrate [14]. Chan and co-workers simulated the dynamics of platinum nanoparticles supported on graphite [15–18] and oxygen adsorption on supported platinum nanoparticles [19]. The distribution of surface and core atoms in platinum nanoparticles was recently discussed [20].

Because of the delocalized electronic character, the interaction between metal atoms cannot be adequately described by pair potentials. It is popular to use a many-body empirical potential in modeling studies of metallic clusters and nanoparticles. The addition of an atom to a small cluster can significantly change the overall structure and energy. In the case of adding a foreign metal to a small metal cluster, the heterogeneity introduces additional complexity.

Mixed-metals are of practical interests such as magnetic and catalytic applications. Recently, bimetallic clusters have been studied by atomistic simulation using many body potentials. Kaszkur and Mierzwa investigated the segregation in Pd–Co clusters [21]. Huang and Balbuena studied the melting of Cu–Ni nanoclusters [22]. Johnston and co-workers studied platinum–palladium and gold–copper bimetallic clusters using the Gupta potential and the genetic algorithm [23–25]. Wang *et al.* studied the structures and magnetic properties of Co–Cu bimetallic clusters [26].

Platinum–cobalt has been used as a mixed metal catalyst in fuel cell electrode reactions [27,28]. In this paper, we apply the many-body SC Potential modified for mixed metal [29] to simulate platinum–cobalt clusters. The basin hopping [30,31]

*Corresponding author. Fax: +852-28571586. E-mail: hrsccky@hku.hk

ISSN 0892-7022 print/ISSN 1029-0435 online © 2004 Taylor & Francis Ltd
DOI: 10.1080/08927020412331279929

algorithm is used to determine the minimum energy structure of clusters of sizes with 11–15 total number of atoms. The change in geometries and energies of the Pt–Co clusters with size and composition will be discussed. In the study of Wales and Doye [11], the icosahedral packing is the predominant structure in SC 9-6 clusters, while SC 10-8 clusters has greater preference for face center cubic (fcc) or close packed structures. So in the SC potential model, platinum and cobalt have different structural behaviors. Pure cobalt nanoparticles show nonperiodic polytetrahedral structures in certain experimental conditions [32]. On the other hand, a pure platinum nanoparticle prefer a fcc arrangement in the bulk state [33–35]. It is interesting to investigate the preferred structure in a platinum–cobalt alloy of the nanoscale. Comparison between Pt–Co and Pt–Pd, Au–Cu and Pd–Co bimetallic clusters will be made. In the study of Johnston *et al.* [23–25], Pt–Pd and Au–Cu are modeled by the Gupta potential, which is a many-body potential, similar to the SC potential. Gold and copper belong respectively, to the same SC families of Pt and Co. The study of Pd–Co cluster modeled by SC potential is a good reference to the discussion about Pt–Co clusters.

COMPUTATIONAL DETAILS

Modified Sutton-Chen Potential

Sutton-Chen potential is also called as long-ranged Finnis-Sinclair (FS) potential, which is a result of the second moment approximation to the tight binding energy [36]. The total internal energy of a pure platinum cluster of N atoms in the SC potential is expressed as

$$U = \varepsilon_{pp} \sum_{i=1}^{N} \left[\frac{1}{2} \sum_{j \neq 1}^{N} \left(\frac{\sigma_{pp}}{r_{ij}} \right)^{n} - c\sqrt{\rho_i} \right] \tag{1a}$$

where N is the total number of atoms, r_{ij} is the separation distance between atoms i and j, c is a dimensionless parameter, ε_{pp} is the energy parameter, σ_{pp} is the lattice constant and m and n are positive integers with $n > m$. Equation (1a) consists of a sum of the pairwise repulsion term and the sum of a many-body density-dependent cohesion term. While electrons are not explicitly included in the potential function, the local density of atoms, ρ_i, is defined as

$$\rho_i = \sum_{j \neq i}^{N} \left(\frac{\sigma_{pp}}{r_{ij}} \right)^{m} \tag{1b}$$

to represent the action of electrons.

The modified SC potential for a binary alloy [29] considers the stoichiometric ratio of two metals, A and B, by introducing the site occupancy operator, with a general formulation of

$$\begin{aligned} U = \frac{1}{2} \Bigg[& \sum\sum_{i \neq j} \hat{p}_i \hat{p}_j V^{AA}(r_{ij}) + (1 - \hat{p}_i)(1 - \hat{p}_j) V^{BB}(r_{ij}) \\ & + [\hat{p}_i(1 - \hat{p}_j) + \hat{p}_j(1 - \hat{p}_i)] V^{AB}(r_{ij}) \Bigg] \\ & - d^{AA} \sum_i \hat{p}_i \left[\sum_{j \neq i} \hat{p}_j \phi^{AA}(r_{ij}) + (1 - \hat{p}_j) \phi^{AB}(r_{ij}) \right]^{1/2} \\ & - d^{BB} \sum_i (1 - \hat{p}_i) \\ & \times \left[\sum_{j \neq i} (1 - \hat{p}_j) \phi^{BB}(r_{ij}) + \hat{p}_j \phi^{AB}(r_{ij}) \right]^{1/2}. \end{aligned} \tag{2a}$$

The occupancy operator works as follows:

$$\begin{aligned} &\hat{p} = 1, \text{ if site } j \text{ is occupied by an A atom.} \\ &\hat{p} = 0, \text{ if site } j \text{ is occupied by a B atom.} \end{aligned} \tag{2b}$$

The occupancy operator $\hat{p}_i$ can degenerate to the simple pure metal SC potential of Eq. (1a). The functions V^{AA}, V^{BB}, V^{AB}, ϕ^{AA}, ϕ^{BB} are defined as

$$\begin{aligned} V^{AA}(r) &= \varepsilon^{AA} \left[\frac{\sigma^{AA}}{r} \right]^{n^{AA}}, \\ V^{BB}(r) &= \varepsilon^{BB} \left[\frac{\sigma^{BB}}{r} \right]^{n^{BB}}, \\ V^{AB}(r) &= \varepsilon^{AB} \left[\frac{\sigma^{AB}}{r} \right]^{n^{AB}}, \\ \phi^{AA}(r) &= \varepsilon^{AA} \left[\frac{\sigma^{AA}}{r} \right]^{m^{AA}}, \\ \phi^{BB}(r) &= \varepsilon^{BB} \left[\frac{\sigma^{BB}}{r} \right]^{m^{BB}}, \\ \phi^{AB}(r) &= \varepsilon^{AB} \left[\frac{\sigma^{AB}}{r} \right]^{m^{AB}}. \end{aligned} \tag{2c}$$

The constants d^{AA}, d^{BB}, are defined as

$$d^{AA} = \varepsilon^{AA} c^{AA} \quad \text{and} \quad d^{AA} = \varepsilon^{BB} c^{BB}. \tag{2d}$$

In the above equations, ε^{AA}, σ^{AA}, c^{AA}, m^{AA} and n^{AA} represent the parameters ε, σ, c, m and n of pure metal A. Similarly ε^{BB}, σ^{BB}, c^{BB}, m^{BB} and n^{BB} represent the parameters ε, σ, c, m and n of pure

TABLE I SC parameters for platinum, cobalt and palladium

Metals	σ (Å)	ε (10^{-2}eV)	C	m	n
Platinum*	3.92	1.9833	34.408	8	10
Cobalt†	3.54	1.5566	39.432	6	9
Palladium‡	3.94	0.4179	108.27	7	12

*Proposed by Sutton and Chen [29]. †Proposed by Kaszkur and Mierzwa [21]. ‡Proposed by Sutton and Chen [29].

metal B. The mixed parameters are expressed as

$$V^{AB} = (V^{AA}V^{BB})^{1/2} \quad \text{and} \qquad \phi^{AB} = (\phi^{AA}\phi^{BB})^{1/2}. \tag{2e}$$

and

$$m^{AB} = \frac{1}{2}(m^{AA} + m^{BB}), \quad n^{AB} = \frac{1}{2}(n^{AA} + n^{BB}), \qquad \sigma^{AB} = (\sigma^{AA}\sigma^{BB})^{1/2}, \quad \varepsilon^{AB} = (\varepsilon^{AA}\varepsilon^{BB})^{1/2}. \tag{2f}$$

The SC parameters for platinum and cobalt are shown in Table I. Bulk cobalt metal normally has a hexagonal close pack (hcp) structure at room temperature but a fcc structure at a higher temperature. Here, we use the fcc SC cobalt parameters, which are recalculated from the parameters of hcp cobalt [21]. Many experimental studies suggested that platinum–cobalt nanoparticles have a fcc structure. Platinum and cobalt are two quite different metals in different families of the SC potential model (different n, m). Platinum is grouped with gold (10-8 family) while cobalt is grouped with copper and nickel (9-6 family).

Basin-hopping Method and Monte Carlo (MC) Simulations

The global optimization with basin-hopping algorithm proposed by Wales and Doye [30,31] was used in the minimum energy structures of the platinum–cobalt clusters. This method has been used efficiently to generate some reliable results [11,30,31,37–48] for Lennard-Jones (LJ) clusters, transition metal clusters, charged rare gas and metal clusters, alkali-ion in rare gas clusters and water clusters. To our knowledge, the basin hopping algorithm has not been applied to bimetallic clusters. In this work, there are three stages of optimization: initial optimization, re-optimization and a basin-hopping optimization with genetic-like operators. In the initial optimization, we use canonical MC sampling at reduced temperatures, $kT/\varepsilon_{Pt} = T^* = 0.0217$ (5K) and $T* = 0.8$ (184.3K). At each temperature, six runs from different random configurations are made with 100,000 MC steps each. Maximum step sizes of 0.75 σ_{Pt} and 0.4 σ_{Pt} were employed in the low temperature and high temperature MC simulations, respectively. The maximum displacement will be adjusted during the simulation, to achieve the acceptance ratio = 0.5.

We use a patient search (simulation with high temperature and small maximum displacement) and an aggressive search (simulation with low temperature and large maximum displacement), alternatively. At the low temperature, we find that the simulation can reach a lower energy minimum without using the convergence criterion based on the value of root-mean-square (RMS) gradient. This may be due to the narrow distribution of energy states. The search would stop until the algorithm cannot find any better structure in that search. Although we have not used the convergence criterion, we still require the RMS gradient of the final results to fall below 10^{-5} in reduced units and the energy change between consecutive steps in the minimization was less than 10^{-5} ε_{Pt}. The final energies are statistically accurate to four decimal places.

The lowest energy structures from the initial optimization are then re-optimized. Two re-optimizations of 20000 MC steps each are performed at a reduced temperature of $T* = 0.8$. A maximum displacement of $0.4\sigma_{Pt}$ is employed. The convergence criterion is applied in one of the re-optimizations. Sloppy quench tolerance and final quench tolerance for RMS gradient are 10^{-4} and 10^{-6}, respectively. In re-optimization, we require the energy change between consecutive steps in the minimization was less than 10^{-8} ε_{Pt}.

After the re-optimization, we undergo final stage of optimization. In order to increase the efficiency in the search of global minima, we introduce two operators into our new scheme of optimization, random exchange operator and mutation operators, which are originally used in the genetic algorithm [24]. Before each optimization step in the new optimization scheme, we randomly move, mutate and exchange the original configuration. In this way, a completely "new" configuration is generated and it can lead to a local minimum, which is far away from the local minimum optimized from previous configuration. It means that we can increase the range of access on the potential energy surface. Compared with classical MC moves in typical basin-hopping algorithm, these two operations help to generate more random configurations and increase the probability of determining the global minima.

In the new scheme of optimization, we start with two sets of seeds (starting configurations). We used the optimized structures from the re-optimization (second stage) to be the first set of seeds of a new optimization. The second set of seeds comes from a random generation. Before the start of optimization, each structure generates fifty offsprings after random exchange and mutation operations. For example, ten optimized structures of 11-atom alloy cluster from re-optimization will generate 500 offspring. Finally, for each offspring, the optimization with 5000 MC moves followed by random

exchange and mutation operation is used to generate the final structures of Pt–Co clusters.

By using the basin-hopping algorithm with two genetic-like operations, we found improved structures of Pt_4Co_{10} and Pt_5Co_9 clusters.

RESULT AND DISCUSSION

11- and 12-atom Pt–Co Clusters

Except for the 12-atom Pt cluster, 11- and 12-atom pure clusters are the fragments of icosahedral 13-atoms clusters, which are so-called pre-icosahedra. For the 11-atom alloy cluster (Fig. 1), adding one or two foreign atoms to the pure metal clusters would not change the atomic arrangements. When the number of foreign atoms increases, the clusters prefer close-packed structures with symmetrical distribution of two types of atoms in cluster. At a low Pt ratio, the clusters show the preference of Pt atoms to come together. The cobalt atoms surround the platinum group. As Pt–Pt interaction is the stronger and the grouping of platinum atoms can minimize the total potential energy of cluster. That is particularly important for the cluster with a low Pt ratio. It seems that the preference of a bond type in the cluster at different atomic ratios is important in determining the lowest energy structure, as shown in Pt_1Co_{10}, Pt_2Co_9, $Pt_{10}Co_1$ and Pt_9Co_2 clusters. They have the same atomic arrangement, but the position of foreign atoms in the cluster is different. For Pt_1Co_{10} and Pt_2Co_9, the first platinum atom is placed at the center of hexagonal surface of cluster and the second platinum atom would be the nearest neighbor of the central platinum atom. For $Pt_{10}Co_1$ and Pt_9Co_2, the cobalt atoms are placed at the edges of the cluster whereas the platinum atoms are at the core positions. Obviously, the formation of Pt–Pt "bonds" has a higher priority than the other "bond" types, especially for the alloy cluster with a low Pt ratio. The formation of a Pt–Pt "bond" can also effectively increase the local density, since the SC local density of each atom is mainly contributed by the nearest neighbors.

For the 11-atom cluster with a low Co ratio, the cobalt atoms tend to disperse at the cluster and locate at the surface of the cluster. This preference can maximize the number of short-range Pt–Pt and Pt–Co interaction in the cluster and increase the total binding energy.

The lowest energy atomic arrangements of pure Pt and Co 12-atoms clusters are different. The pure Co cluster is of an incomplete icosahedron while the Pt cluster has a less symmetrical and close-packed structure with a hexagonal pattern. Of all the atomic combinations of 12-atom Pt–Co clusters (Fig. 2), seven of them follow the structure of a pure Co cluster and none of them has the structure resemble a pure Pt cluster. The structures of Pt_3Co_9, Pt_4Co_8, Pt_5Co_7 and $Pt_{10}Co_2$ clusters are based on that of Pt_3Co_8, Pt_4Co_7, Pt_5Co_6 and Pt_9Co_2, respectively.

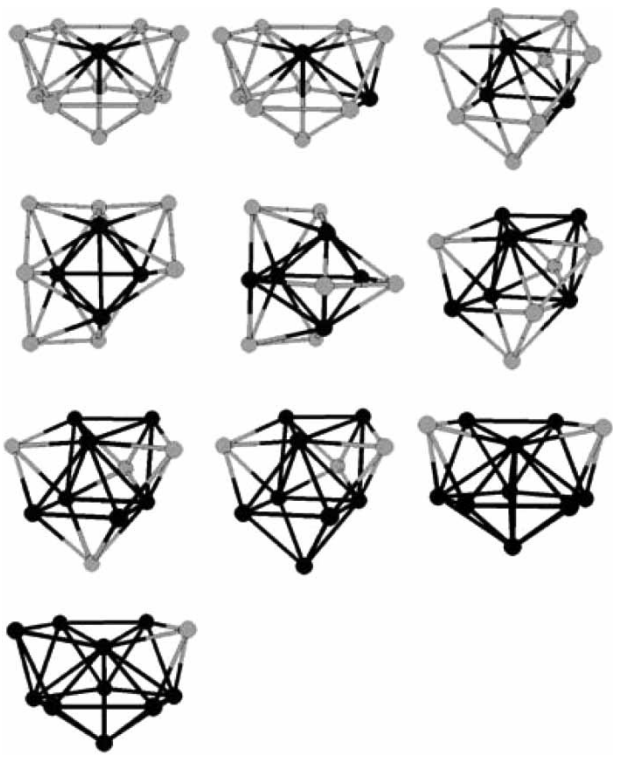

FIGURE 1 Structure of global minima for 11-atom platinum–cobalt clusters. (Platinum and cobalt atoms in black).

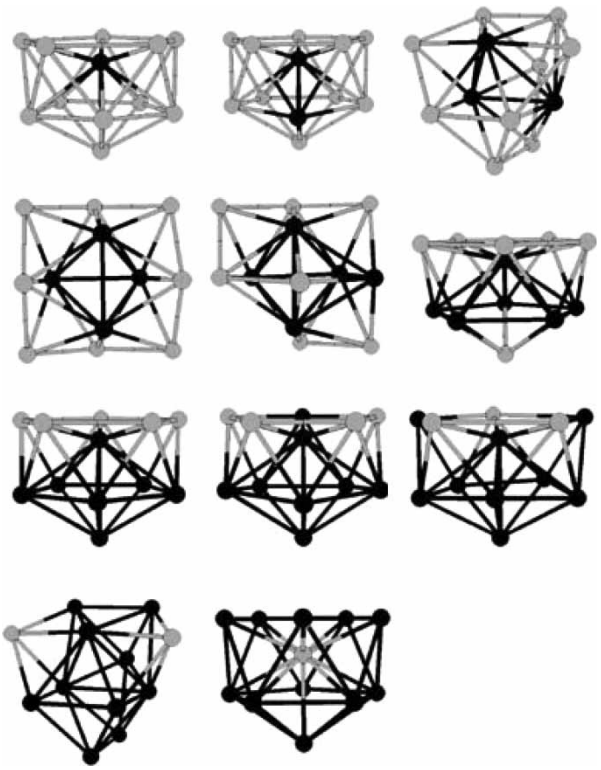

FIGURE 2 Structure of global minima for 12-atom platinum–cobalt clusters.

The two kinds of atoms are also symmetrically distributed in the clusters and segregation is observed.

For 12-atom Pt–Co clusters with incomplete icosahedral structures, segregation also occurs. For example, in Pt_6Co_6, Pt_7Co_5, and Pt_8Co_4, the cobalt atoms are placed at the top plane of the cluster and platinum atoms get together at the base. Also, there is a cobalt atom at the bottom of the Pt_6Co_6 cluster to maximize the short range Pt–Co interaction of five platinum atoms. When the Pt_6Co_6 cluster changes to the Pt_7Co_5 cluster, the cobalt atom at the bottom is replaced by a platinum atom and five new Pt–Pt bonds are formed. In this replacement of atoms, the increase in binding energy can be maximized.

13-atom Pt–Co Clusters

In many experimental and theoretical investigations of rare gas and metal clusters, 13-atom clusters are usually arranged as an icosahedron. Recently, some theoretical studies suggested that some 13-atom pure metallic clusters have amorphous structures [49]. From our results, most 13-atom alloy clusters (Fig. 3) are arranged in icosahedrons, but some of them (Pt_3Co_{10}, Pt_4Co_9 and Pt_5Co_8) are non-icosahedral structures. The energy minimum structure of Pt_3Co_{10} is a distorted icosahedron, with two vertices and one central Pt atom. Pt_4Co_9 and Pt_5Co_8 are fragments of platinum atom containing icosahedrons with attachment of cobalt atoms. Clearly, the alloying effect can change the atomic arrangement to prefer formation of the stronger Pt–Pt and Pt–Co bonds. For Pt_1Co_{12} and $Pt_{12}Co_1$, the foreign atom was placed at the center of clusters and there are one vertex and one central foreign atom in Pt_2Co_{11} and $Pt_{11}Co_2$ clusters. This arrangement can maximize the number of Pt–Co bond. Pt_6Co_7, Pt_7Co_6, Pt_8Co_5 and Pt_9Co_4 clusters also show the segregation as mentioned in the previous section. But the atoms tend to form layered structures, instead of two regions of platinum and cobalt atoms.

14- and 15-atom Pt–Co Clusters

In all combinations of 14-atom and 15-atom Pt–Co clusters (Figs. 4 and 5), we find that most of the clusters have structures based on the icosahedral packing. Starting from $Pt = 6$ in 14-atom and 15-atom clusters, all of the structures are based on icosahedral packing. In these icosahedral 14- and 15-atom Pt–Co clusters, all the central atoms are cobalt atoms, even when platinum is the minor atom.

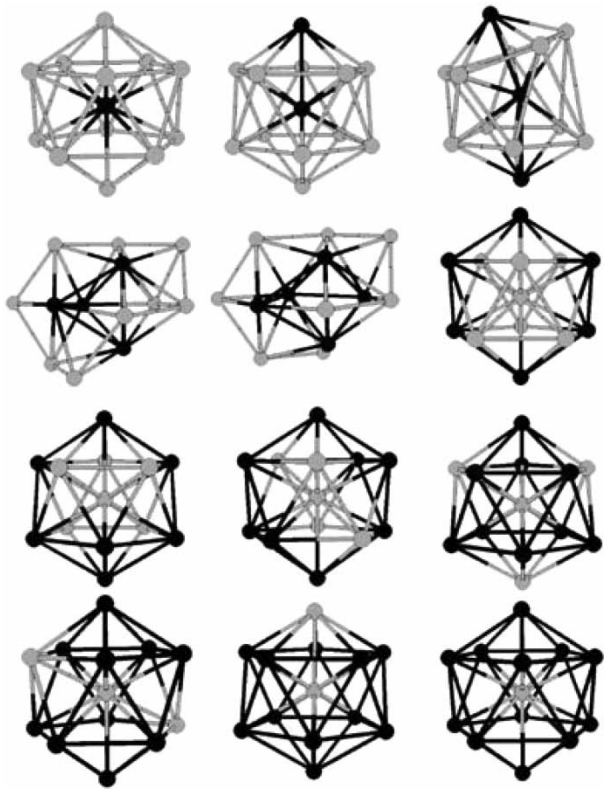

FIGURE 3 Structure of global minima for 13-atom platinum–cobalt clusters.

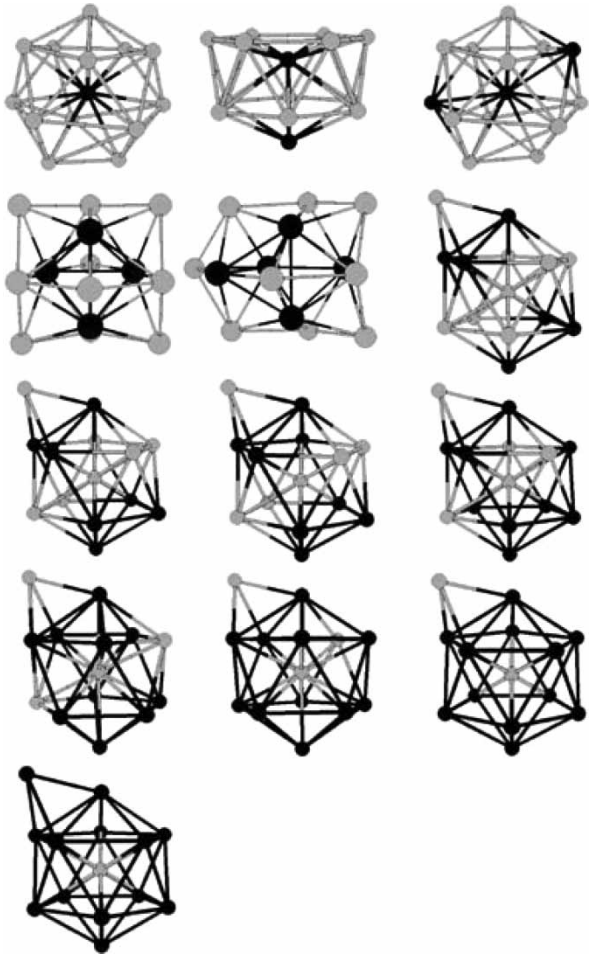

FIGURE 4 Structure of global minima for 14-atom platinum–cobalt clusters.

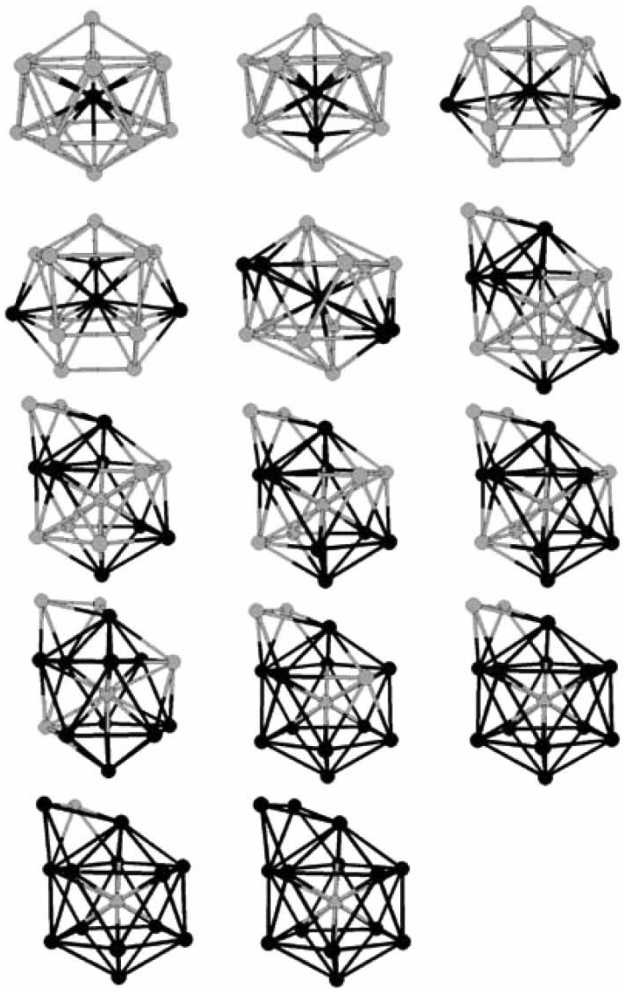

FIGURE 5 Structure of global minima for 15-atom platinum–cobalt clusters.

Probably, the central Co atom can shorten the bond lengths inside the icosahedron and increase the binding energy. The other combinations of 14-atom and 15-atom clusters have structures of polyhedron, distorted decahedron and incomplete icosahedron. This result is interesting because icosahedron is not a favorable structure in the 10-8 SC potential for Pt, compared with the 9-6 potential [11]. Also, for pure 14- and 15-platinum and cobalt clusters, only the pure 14-atom cobalt cluster has an icosahedral structure. The 15-atom cobalt cluster is one of the Frank-Kasper coordination polyhedra. The 14-atom platinum cluster has one of the seven-coordinate vertices removed and the 15-atom cluster is a distorted decahedron. So the dominant icosahedral structures in 14- and 15-atom Pt–Co clusters, especially at higher Pt ratio, are unexpected. From this, it seems that the minor atoms (the atom which has lower atomic ratio in an alloy cluster) in a Pt–Co cluster would govern the structural arrangement, as the icosahedral packing is more favorable in 9-6 SC cluster, compared with 10-8 cluster. A similar phenomenon was also found by Johnston *et al.* [24] and Lopez *et al.* [50], in which the replacement of one gold atom by copper is sufficient to convert the structure to that of the more symmetrical copper cluster. Actually, the tendency of formation of mixed bond may account for this. As the icosahedron is a highly symmetrical structure, so that placing the foreign atom at the central position of the icosahedron can fully maximize the number of Pt–Co bond in the cluster. In general, all of the alloy clusters in this study are based on icosahedral packing. At low Pt ratio, small alloy clusters tend to maximize the number of Pt–Pt bonds and form platinum group or layered structure, in order to increase the binding energy.

Compared to the other theoretical study of alloy clusters, we found some similarity between the study of Pt–Pd alloy clusters and Pt–Co clusters in our study. Although Johnston *et al.* [23] mainly focused on the study of $(PtPd)_m$ bimetallic clusters, 14-atom cluster was used to investigate the variation in the geometric structure of the global minima as a function of composition. They found when Pt atoms are substituted by Pd atoms, the capped icosahedral structure can be kept. The Pd atoms are in the capping site while the Pt atoms are at the interstitial sites. For the result of 14-atom Pt–Co clusters, the icosahedral structures also dominate in Pt-rich alloy clusters, but the cobalt atoms occupies the central position of the icosahedral packing, rather than the platinum atoms. This difference can be accounted by the order of attractive and repulsive parts for different metals in SC potential. In SC potential, the parameters for Pd are also provided, as shown in Table I. Palladium has the order of attractive term close to that of cobalt (7 for Pd and 6 for Co), but their repulsive terms have large difference (12 for Pd and 9 for Co). This means that if the palladium atom is placed at the central position of an icosahedron, it will experience much larger repulsive interaction with the surface atoms than the cobalt atom. Also, the size of cobalt atom is smaller than palladium (lattice constant of Co and Pd is 3.54 and 3.89 Å, respectively) and the central atom with smaller size can effectively reduce the bulk strain in an icosahedron [23].

On the other hand, Johnston *et al.* [24] also found that the central atom of icosahedron-based Au–Cu clusters is usually a copper atom at different atomic ratios. They account that the smaller copper atom at central position can let the atoms get closer and increase the binding energy. But in our study, the central cobalt atoms are found to be favorable in icosahedral packing, while the central platinum atoms are favorable in decahedral packing. So we can conclude that smaller cobalt atom is particular important to stabilize the icosahedral packing, by placing at the central position.

As the icosahedral packing has a high degree of symmetry, if a cobalt atom is placed at the central

position of an icosahedral platinum cluster, the bond distance between central and surface atoms would have the same extent of contraction. As a result, all surface atoms would get closer to the central atoms.

Energy Analysis of Global Minima and Size Dependent Evolution of Bimetallic Clusters

The investigation of energy of global minima is also important for us to understand the structural variation of cluster at different sizes and compositions. Table II shows all global minima (eV per atom) of Pt–Co bimetallic clusters. All the energy values of *N*-atom alloy cluster are in between that of pure *N*-atom cobalt and platinum clusters. For the first three rows, the energy increases from left to right. But for the other rows, the energy decreases from left to right. For the first three rows, the starting clusters contain zero, one and two platinum atoms, respectively. Cobalt atom is added one by one into the starting cluster and overall binding energy and the energy per atom in cluster increase from left to right in the table. Although adding cobalt atoms also increase the overall binding energy in the other rows, the energy per atom decreases from left to right. In other words, adding cobalt atom would destabilize these starting clusters. The difference in the trend of energy per atom observed is caused by different atomic ratios in starting clusters. When all or most of the atoms in the starting cluster are cobalt atoms, the energy per atom is relatively low. Adding cobalt atoms in these clusters would effectively increase the energy per atom and that is similar to the case of a pure cobalt cluster. If there are more platinum atoms in starting clusters, the energy per atom is relatively high, adding more and more low energy cobalt atoms would lower the energy per atom.

For all of the columns, the energy increases from the top to bottom. Keeping the number of cobalt atoms constant in the starting cluster, platinum atom is added one by one into the starting cluster and overall binding energy and energy per atom are efficiently increased.

Binding energy of global minima at different compositions and sizes can reflect their relative stability. The second energy difference is the most common method to analyze the energy of metal and alloy cluster. In our work, this method was modified to give a more appropriate account for the energies of bimetallic clusters.

Modified Second Energy Difference (I)

Original second energy difference is often used to analyze the stability of a structure with respect to neighboring sizes. The typical form of second energy

TABLE II Global minima of Pt–Co bimetallic clusters (eV per atom)

Pt/Co	*0*	*1*	*2*	*3*	*4*	*5*	*6*	*7*	*8*	*9*	*10*	*11*	*12*	*13*	*14*	*15*
0												−3.259	−3.298	−3.364	−3.362	−3.391
1											−3.481	−3.497	−3.524	−3.532	−3.562	
2										−3.655	−3.653	−3.661	−3.663	−3.681		
3									−3.828	−3.822	−3.800	−3.796	−3.804			
4								−3.990	−3.965	−3.937	−3.924	−3.921				
5							−4.143	−4.107	−4.070	−4.054	−4.034					
6						−4.278	−4.242	−4.205	−4.169	−4.147						
7					−4.425	−4.371	−4.332	−4.288	−4.260							
8				−4.556	−4.494	−4.456	−4.405	−4.371								
9			−4.689	−4.613	−4.581	−4.518	−4.474									
10		−4.815	−4.736	−4.704	−4.631	−4.579										
11	−4.942	−4.861	−4.823	−4.740	−4.681											
12	−4.968	−4.944	−4.851	−4.784												
13	−5.004	−4.946	−4.879													
14	−5.028	−4.974														
15	−5.057															

difference is given as:

$$E_{\text{diff}}(n) = E(n+1) + E(n-1) - 2E(n) \qquad (3)$$

$E(n)$, $E(n+1)$ and $E(n-1)$ are the total binding energies of n, $n+1$ and $n-1$ atom clusters, respectively. This method is widely accepted to investigate the relationship between the energy and sizes of clusters. The peak in second energy difference plot has been found to correlate well the magic numbers of alkali metal clusters [51]. But the second energy difference in this form may not be most representative. So we modified the second energy difference with the consideration of energy per atom:

$$E(n)/n = [E(n+1)/(n+1)] + [E(n-1)/(n-1)] - 2[E(n)/n] \qquad (4)$$

In this approach, we consider the difference in average energy per atom at different cluster sizes. This can give a better account for the relative stabilities of cluster with respect to neighboring sizes as compositions. All energy terms are normalized accordingly.

Modified Second Energy Difference (II)

When we calculate the second energy difference of Pt_mCo_n, all the neighboring clusters of a particular cluster in table of energy is considered in the calculation:

$$E_{\text{diff}}(Pt_mCo_n) = \sum E(\text{All neighboring clusters}) - (\text{No. of neighboring clusters}) \times E(Pt_mCo_n) \qquad (5)$$

Analysis of the second energy difference in this way helps us to explore the relative stability between the particular cluster in the table of energy and its neighboring clusters.

Figures 6–9 show the type I second energy difference with increasing size of alloy cluster. Starting from 11-atom alloy clusters, platinum (Figs. 6 and 8) and cobalt (Figs. 7 and 9) atoms were added respectively, until the total number of atoms in alloy cluster is 15. From the figures, we found that different starting clusters would have different changes of energy with size. When platinum and cobalt atoms are added, the starting clusters with a high Pt content (Figs. 8 and 9) cause a sharp peak when total number of atoms in alloy cluster is equal to 13. A peak in the plot of second energy difference represents higher stability compared with the neighboring sizes. For Pt_7Co_4, Pt_8Co_3, Pt_9Co_2 and $Pt_{10}Co_1$, adding platinum atoms into the cluster causes greater second energy difference, compared with the addition of cobalt atoms. This indicates that the higher the Pt content, the higher is the relative stability the 13-atom alloy clusters.

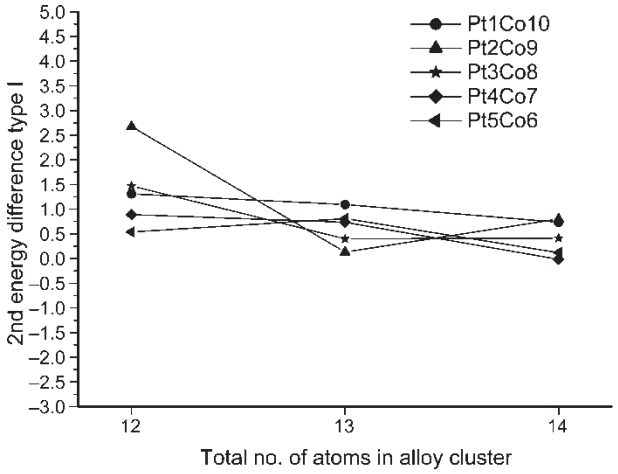

FIGURE 6 Second energy difference type I with increasing Pt–Co cluster size by adding Pt atoms. The starting clusters are Pt_1Co_{10}, Pt_2Co_9, Pt_3Co_8, Pt_4Co_7 and Pt_5Co_6, respectively.

At a low Pt (high Co) content, some of the clusters, which are non-icosahedral (e.g. Pt_5Co_8 and Pt_4Co_9), show lower stability at $N = 13$, compared with the neighboring sizes. This indicates that the highly symmetrical icosahedral geometry is important to the stability of 13-atom alloy clusters. Compared with the second energy difference plots by Doye and Wales [11], where a sharp peak was at $N = 13$ in pure 9-6 SC clusters, there is only a small peak at $N = 13$ in pure 10-8 SC clusters. Both of 9-6 and 10-8 SC 13-atom clusters are icosahedra. This indicates 9-6 (cobalt) icosahedral cluster has higher stability than 10-8 (platinum) icosahedral cluster. The difference in stabilities of 10-8 and 9-6 icosahedral clusters can be explained by the ranges of 10-8 and 9-6 SC potentials.

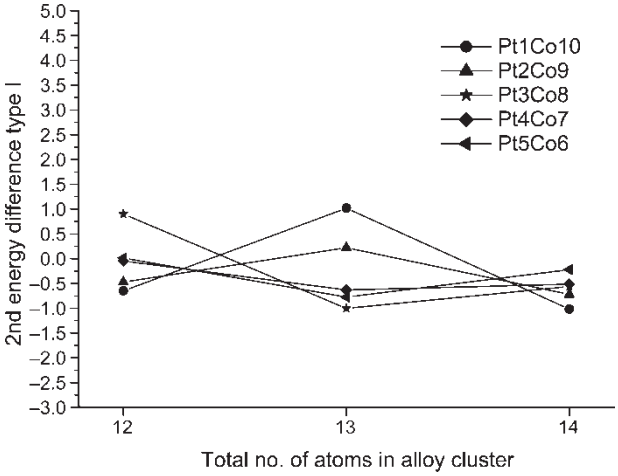

FIGURE 7 Second energy difference type I with increasing Pt–Co cluster size by adding Co atoms. The starting clusters are Pt_1Co_{10}, Pt_2Co_9, Pt_3Co_8, Pt_4Co_7 and Pt_5Co_6, respectively.

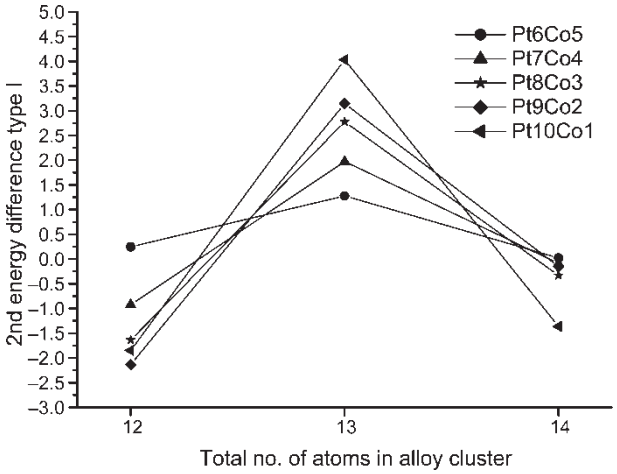

FIGURE 8 Second energy difference type I with increasing Pt–Co cluster size by adding Pt atoms. The starting clusters are Pt_6Co_5, Pt_7Co_4, Pt_8Co_3, Pt_9Co_2 and $Pt_{10}Co_1$, respectively.

In the study of Doye and Wales, the SC potentials with a longer range (12-6 and 9-6) cause the stronger preference of icosahedral arrangement, while SC potential with a shorter range (10-8) causes the stronger preference of close packed structures. Although the pure platinum 13-atom cluster is icosahedral, the structural preference of 10-8 potential causes the lower stability of icosahedral cluster, compared with pure cobalt cluster. So it is expected that more cobalt atoms would give a higher stability to the icosahedral alloy cluster. But in our study, we find that the stability of 13-atom icosahedral alloy cluster decreases in stability with increasing number of cobalt atoms. This can be explained by the atomic arrangement of two species in icosahedral cluster. From the plot, we know that $Pt_{12}Co_1$ is the most stable icosahedral alloy cluster. Its stability actually comes from the central cobalt atom. This cobalt atom lets the platinum atoms get closer and effectively maximizes the binding energy. But if one platinum atom in $Pt_{12}Co_1$ is replaced by a cobalt atom and form $Pt_{11}Co_2$, stability would then decrease. Although a cobalt atom at the central position of icosahedron can increase the relative stability, more and more cobalt atoms would lower the stability of cluster. This is caused by two reasons. First, more and more cobalt would lower the overall binding energy. The other reason is that replacing the surface platinum atoms in an icosahedral cluster would disturb the atomic arrangement and break down the high symmetry of cluster.

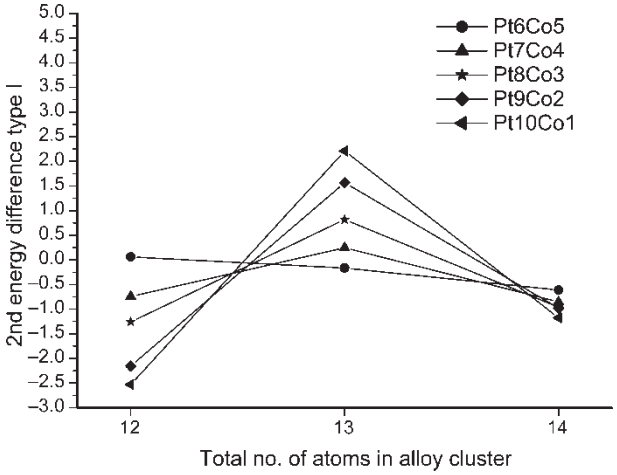

FIGURE 9 Second energy difference type I with increasing Pt–Co cluster size by adding Co atoms. The starting clusters are Pt_6Co_5, Pt_7Co_4, Pt_8Co_3, Pt_9Co_2 and $Pt_{10}Co_1$, respectively.

Other than the simple size effect, the type of atoms (platinum and cobalt) added into an alloy cluster also governs the energy variation. From the plots of second energy difference type I with increasing cluster size by adding platinum atoms (Figs. 6 and 8), all of the second energy differences are positive, except the 12- and 14-atom alloy cluster starting from Pt_7Co_4, Pt_8Co_3, Pt_9Co_2 and $Pt_{10}Co_1$. The negative second energy difference of 12- and 14-atom alloy cluster is due to the special stability of icosahedral 13-atom clusters. For the 14-atom alloy clusters, the value of second energy difference decreases with increasing Pt content of starting clusters. Overall, during the alloy cluster growth, adding platinum atoms forms energetically stable clusters.

On the other hand, with increasing the Pt content in the starting cluster, trends of decreasing value of second energy difference during platinum atom addition are observed at $N = 14$. The possible reason for this is particularly high stability of icosahedral 13-atom alloy cluster with high Pt content. Addition of extra atoms into these clusters would distort them. As a result, relatively unstable alloy clusters are formed.

The second energy difference type II can give us idea about relative stability of all alloy cluster, compared with all the neighboring clusters with different sizes and compositions. Table III shows the map of second energy difference type II. The more positive the value of the particular alloy cluster, the higher relative stability the cluster has.

For 13-atom alloy clusters, Pt_3Co_{10}, Pt_4Co_9 and Pt_5Co_9 are relatively unstable than the other combinations. It may be due to the non-icosahedral geometry of these alloy clusters. The 14-atom alloy clusters have lower stability, as the additional atom to the 13-atoms alloy clusters would cause distortion of the highly symmetrical arrangement. Compared with the type I, second energy difference type II can give a clearer picture about the relative stability of alloy clusters, as the atomic composition of alloy cluster is also considered. That is important for us to study the energetic properties of alloy clusters.

TABLE III Second energy difference (Type II) of Pt–Co bimetallic clusters (10^{-3} eV per atom)

Pt/Co	1	2	3	4	5	6	7	8	9	10	11	12	13
1											100.6	131.5	39.73
2										3.629	31.24	−14.78	
3									99.30	1.909	2.950		
4								27.09	−4.286	6.359			
5							24.87	−8.007	18.47				
6						19.02	17.57	−2.487					
7					−4.999	21.97	−16.76						
8				−39.77	42.90	−13.94							
9			−76.38	71.84	−16.56								
10		−97.32	102.8	−23.11									
11	−62.20	107.9	−30.03										
12	206.7	−14.74											
13	−7.219												

CONCLUSIONS

Small platinum cobalt bimetallic clusters ($N = 11–15$) were modeled by the many-body SC potential. Basin-hopping algorithm and MC energy minimization were used to search the global minima. The limited size range of platinum–cobalt is studied as the ability of basin-hopping simulation to locating global minima decreases with the increasing size of system [30]. Furthermore, the case of alloy system is much more complicated than the pure metal one and provide more possibility of structural configurations. As a result, we present the result at a limited size range in this paper. More efficient searching method is desired to finding the global minima of larger size of platinum–cobalt bimetallic clusters.

The icosahedral packing dominates at this cluster size range in our study. Minor atoms play an important role in the structural arrangement of a bimetallic cluster. A single foreign atom is sufficient to change the structure of some clusters. At a low Pt ratio, the smaller alloy clusters in the study tend to maximize the number of Pt–Pt bonds and form small platinum groups, in order to increase the binding energy.

Modified second energy difference type I and II were used to analyze the relative stability of cluster compared with neighboring sizes and compositions. We found that different starting clusters have different changes of energy with size. For high Pt content of starting cluster, the second energy difference type I analysis shows a sharp peak when total number of atoms in alloy cluster is equal to 13. The peak level decreases with the Pt content and this indicates that the higher the Pt content (the lower the Co content), the higher relative stability the 13-atom alloy clusters would have. It is probably due to the stabilizing effect of minor cobalt atom in icosahedral packing. Other than the simple size effect, the type of atoms (platinum and cobalt) added into an alloy cluster also governs the energy variation. During the alloy cluster growth by adding platinum atoms, most of the second energy differences type I are positive. Overall, this indicates that addition of platinum atoms form an energetically stable cluster. On the other hand, addition of cobalt atoms destabilizes the alloy cluster, as half of the clusters give negative second energy differences.

Table III shows that 14-atom alloy clusters have a lower stability, as the adding an atom to the 13-atom alloy clusters would cause distortion of the highly symmetrical arrangement.

In this work, we used a semi-empirical and many-body SC potential to model platinum–cobalt bimetallic clusters. This potential does not contain the directional terms and might have predicted excessive surface relaxations [52]. But in the same study, the SC potential is proved to correctly predict

the trend of surface energies of different types of metals, which is important for us to predict the mixing of platinum and cobalt in a nanocluster with high amount of surface atoms.

The treatment of interaction in Pt–Co alloy by using ab-initio or Car-Parrinello molecular dynamics approached but would demand extensive computational power. Recently, ab-initio modeling of Pt–Co alloy in bulk state [53] has been performed. As the fundamental knowledge of small Pt–Co cluster is limited, so present study may be a starting point to investigate the nano-alloying of platinum and cobalt and provide some valuable information for other experimental and theoretical studies in the future.

Acknowledgements

Y.H. Chui acknowledges a studentship from the University of Hong Kong for his postgraduate study. The authors also thank Dr David Wales (University of Cambridge, UK) for access to GMIN (Basin-hopping global optimization) program and Professor S.K. Lai (National Central University, Taiwan) for useful discussion on this project. This work was funded by the Research Grant Council of Hong Kong (HKU 7072/01P).

References

[1] Dereli, G., Cagin, T., Uludogan, M. and Tomak, M. (1997) "Thermal and mechanical properties of Pt–Rh alloys", *Philos. Mag. Lett.* **75**, 209.
[2] Qi, Y., Cagin, T., Kimura, Y. and Goddard, W.A., III. (1999) "Molecular-dynamics simulations of glass formation and crystallization in binary liquid metals: Cu–Ag and Cu–Ni", *Phys. Rev. B* **59**, 3527.
[3] Dereli, G., Cagin, T., Uludogan, M. and Tomak, M. (1999) "Thermal and mechanical properties of some fcc transition metals", *Phys. Rev. B* **59**, 3468.
[4] Qi, Y., Cagin, T., Kimura, Y. and Goddard, W.A., III. (2001) "Melting and crystallization in Ni nanoclusters: the mesoscale regime", *J. Chem. Phys.* **115**, 385.
[5] Nayak, S.K., Reddy, B., Rao, B.K., Khanna, S.N. and Jena, P. (1996) "Structure and properties of Ni-7 cluster isomers", *Chem. Phys. Lett.* **253**, 390.
[6] Nayak, S.K., Khanna, S.N., Rao, B.K. and Jena, P. (1997) "Physics of nickel clusters: energetics and equilibrium geometries", *J. Phys. Chem. A* **101**, 1072.
[7] Nayak, S.K., Khanna, S.N., Rao, B.K. and Jena, P. (1998) "Thermodynamics of small nickel clusters", *J. Phys.: Condens. Matter* **10**, 10853.
[8] Uppenbrink, J. and Wales, D.J. (1992) "Structure and energetics of model metal clusters", *J. Chem. Phys.* **11**, 8520.
[9] Uppenbrink, J. and Wales, D.J. (1993) "Structure and dynamics of model Ag and Pt clusters", *Z. Phys. D* **26**, 258.
[10] Munro, L.J. and Wales, D.J. (1996) "Changes of morphology and capping of model transition metal clusters", *J. Phys. Chem.* **100**, 2053.
[11] Doye, K.J.P. and Wales, D.J. (1998) "Global minima for transition metal clusters described by Sutton-Chen potentials", *New. J. Chem.*, 733.
[12] Shiang, K.D. (1993) "Theoretical studies of adatom diffusion on metal surfaces", *Phys. Lett.* **180**, 444.
[13] Shiang, K.D., Wei, C.M. and Tsong, T.T. (1994) "A molecular dynamics study of self diffusion on metal surfaces", *Surf. Sci.* **301**, 136.
[14] Huang, S.P. and Balbuena, P.B. (2002) "Platinum nanoclusters on graphite substrates: a molecular dynamics study", *Mol. Phys.* **100**, 2165.
[15] Liem, S.Y. and Chan, K.Y. (1995) "Effective pairwise potential for simulations of adsorbed platinum", *Mol. Phys.* **86**, 939.
[16] Liem, S.Y. and Chan, K.Y. (1995) "Simulation study of platinum adsorption on graphite using the Sutton-Chen potential", *Surf. Sci.* **328**, 119.
[17] Wu, G.W. and Chan, K.Y. (1996) "Morphology of platinum clusters on graphite at different loadings", *Surf. Sci.* **365**, 38.
[18] Wu, G.W. and Chan, K.Y. (1997) "Molecular simulation of platinum clusters on graphite", *Surf. Rev. Lett.* **4**, 855.
[19] Wu, G.W. and Chan, K.Y. (1998) "Molecular simulation of oxygen on supported platinum clusters", *J. Electroanal. Chem.* **450**, 225.
[20] Chui, Y.H. and Chan, K.Y. (2003) "Analyses of surface and core atoms in a platinum nanoparticle", *Phys. Chem. Chem. Phys.* **5**, 2869.
[21] Kaszkur, Z.A. and Mierzwa, B. (1998) "Segregation in model palladium–cobalt clusters", *Philos. Mag. A* **77**, 781.
[22] Huang, S.P. and Balbuena, P.B. (2002) "Melting of bimetallic Cu–Ni nanoclusters", *J. Phys. Chem. B* **106**, 7225.
[23] Massen, C., Mortimer-Jones, T.V. and Johnston, R.L. (2002) "Geometries and segregation properties of platinum–palladium nanoalloy clusters", *J. Chem. Soc., Dalton Trans.*, 4375.
[24] Darby, S., Mortimer-Jones, T.V., Johnston, R.L. and Roberts, C.J. (2002) "Theoretical study of Cu–Au nanoalloy clusters using a genetic algorithm", *J. Chem. Phys.* **116**, 1536.
[25] Wilson, N.T. and Johnston, R.L. (2002) "A theoretical study of atom ordering in copper–gold nanoalloy clusters", *J. Mater. Chem.* **12**, 2913.
[26] Wang, J., Wang, G., Chen, X., Lu, W. and Zhao, J. (2002) "Structure and magnetic properties of Co–Cu bimetallic clusters", *Phys. Rev. B* **66**, 014419.
[27] Chi, N., Chan, K.-Y. and Phillips, D.L. (2001) "Electrocatalytic oxidation of formic acid by Pt/Co nanoparticles", *Catalysis Lett.* **71**, 21.
[28] Zhang, X. and Chan, K.Y. (2002) "Microemulsion synthesis and electrocatalytic properties of platinum–cobalt nanoparticles", *J. Mater. Chem.* **12**, 1203.
[29] Rafii-Tabar, H. and Sutton, A.P. (1991) "Long-range Finnis-Sinclair potentials for fcc metallic alloys", *Philos. Mag. Lett.* **63**, 217.
[30] Wales, D.J. and Doye, J.P.K. (1997) "Global optimization by basin-hopping and the lowest energy structures of Lennard-Jones clusters containing up to 110 atoms", *J. Phys. Chem. A* **101**, 5111.
[31] Wales, D.J. and Scheraga, H.A. (1999) "Review: chemistry—global optimization of clusters, crystals, and biomolecules", *Science* **285**, 1368.
[32] Dassenoy, F., Casanove, M.-J., Lecante, P., Verelst, M., Snoeck, E., Mosset, A., Ould Ely, T., Amiens, C. and Chaudret, B. (2000) "Experimental evidence of structural evolution in ultrafine cobalt particles stabilized in different polymers—from a polytetrahedral arrangement to the hexagonal structure", *J. Chem. Phys.* **112**, 8137.
[33] Ahamdi, T.S., Wang, Z.L., Henglein, A. and El-Sayed, M.A. (1996) ""Cubic" colloidal platinum nanoparticles", *Chem. Mater.* **8**, 1161.
[34] Fu, X., Wang, Y., Wu, N., Gui, L. and Tang, Y. (2001) "Surface modification of small platinum nanopclusters with alkylamine and alkythiol: an XPS study on the influence of organic ligands on the Pt 4f binding energies of small platinum nanoclusters", *J. Colloid Interface Sci.* **243**, 326.
[35] Perez, H., Pradeau, J.P., Albouy, P.-A. and Perez-Omil, J. (1999) "Synthesis and characterization of functionalized platinum nanoparticles", *Chem. Mater.* **11**, 3460.
[36] Finnis, M.W. and Sinclair, J.E. (1984) "A simple empirical n-body potential for transition metals", *Philos. Mag. A* **50**, 45.
[37] Cavlo, F., Tran, S., Blundell, A., Guet, C. and Spiegelmann, F. (2000) "Three-dimensional global optimization of Nan+ sodium clusters in the range $n <= 40$", *Phys. Rev. B* **62**, 10394.
[38] Bilalbegovic, G. (2003) "Alkali-metal ion in rare gas clusters: global minima", *Phys. Lett. A* **308**, 61.
[39] Munro, L.J., Tharrington, A. and Jordan, K.D. (2002) "Global optimization and finite temperature simulations of atomic

clusters: use of XenArm clusters as test systems", *Com. Phys. Comm.* **145**, 1.
[40] Lai, S.K., Hsu, P.J., Wu, K.L., Liu, W.K. and Iwamatsu, M. (2002) "Structures of metallic clusters: mono- and polyvalent metals", *J. Chem. Phys.* **117**, 10715.
[41] Naumkin, F.Y. and Wales, D.J. (2002) "Diatomics-in-molecules potentials incorporating *ab initio* data: application to ionic, Rydberg-excited, and molecule-doped rare gas clusters", *Comp. Phys. Comm.* **145**, 141.
[42] Doye, J.P.K., Wales, D.J., Branz, W. and Calvo, F. (2001) "Modeling the structure of clusters of C-60 molecules", *Phys. Rev. B* **64**, 235409.
[43] Leary, R.H. (2000) "Global optimization on funneling landscapes", *J. Global Optim.* **18**, 367.
[44] Tanaka, H. (2000) "Potential energy surfaces of supercooled water: intrabasin and interbasin structures explored by quenching, normal mode excitation, and basin hopping", *J. Chem. Phys.* **113**, 11202.
[45] Hodges, M.P. and Wales, D.J. (2000) "Global minima of protonated water clusters", *Chem. Phys. Lett.* **324**, 279.
[46] Calvo, F. and Spiegelmann, F. (2000) "Mechanisms of phase transitions in sodium clusters: From molecular to bulk behavior", *J. Chem. Phys.* **112**, 2888.
[47] Naumkin, F.Y. and Wales, D.J. (1998) "Structure and properties of Ne-n(+) clusters from a diatomics-in-molecules approach", *Mol. Phys.* **93**, 633.
[48] Leary, R.H. and Doye, J.P.K. (1999) "Tetrahedral global minimum for the 98-atom Lennard-Jones cluster", *Phys. Rev. E* **60**, R6320.
[49] Oviedo, J. and Palmer, R.E. (2002) "Amorphous structures of Cu, Ag, and Au nanoclusters from first principles calculations", *J. Chem. Phys.* **117**, 9548.
[50] Lopez, M.J., Marcos, P.A. and Alonso, J.A. (1995) "Structural and dynamical properties of Cu–Au bimetallic clusters", *J. Chem. Phys.* **104**, 1056.
[51] Knight, W.D., Clemenger, K., de Heer, W.A., Saunders, W.A., Chou, M.Y. and Cohen, M.L. (1984) "Electronic shell structure and abundances of sodium clusters", *Phys. Rev. Lett.* **52**, 2141.
[52] Todd, B.D. and Lynden-Bell, R.M. (1993) "Surface and bulk properties of metals modeled with Sutton-Chen potentials", *Surf. Sci.* **281**, 191.
[53] Lee, Y.S., Rhee, J.Y., Whang, C.N. and Lee, Y.P. (2003) "Electronic structure of Co–Pt alloys: X-ray spectroscopy and density-functional calculations", *Phys. Rev. B* **68**, 235111.